

Developing a Microfluidic Nozzle to Generate Water Sheet Jets for Cooling Sharp Leading Edges

Priyanka Sinha

Thermo-Fluids and Interfaces Lab, Faculty of Aerospace Engineering
Technion – Israel Institute of Technology

MSc Research seminar

Under the supervision of Asst. Prof. Alexandros Terzis


Thermo Fluids
& Interfaces Lab



**DEPARTMENT OF
AEROSPACE ENGINEERING**

TECHNION
Israel Institute
of Technology

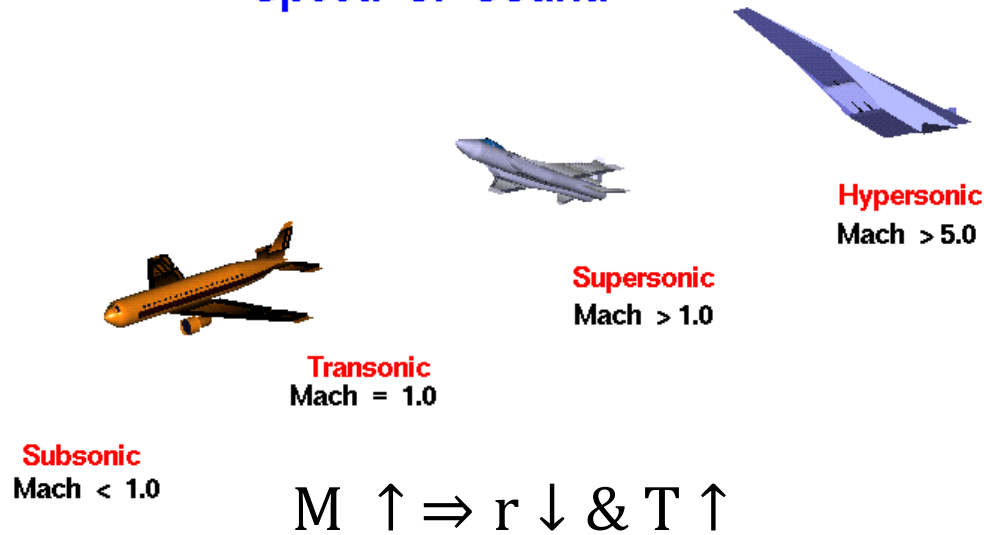
Hypersonic flight and aerodynamic heating



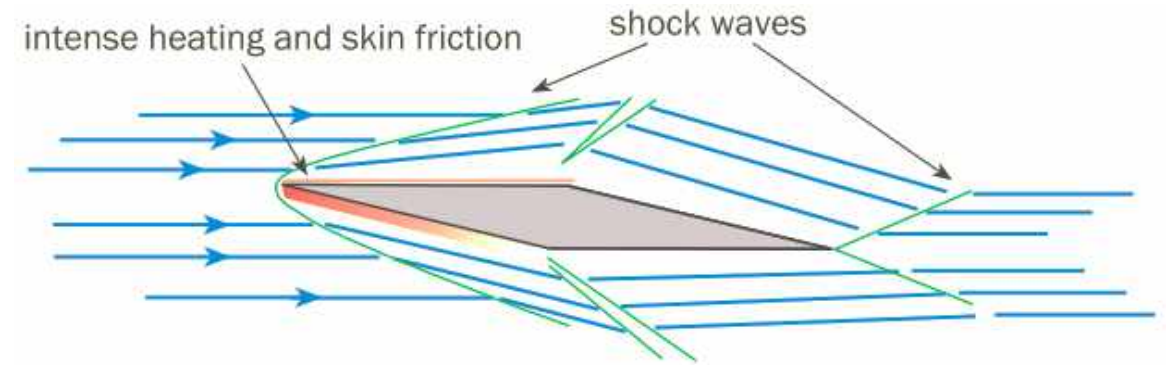
Mach Number

Glenn
Research
Center

$$\text{ratio} = \frac{\text{Object Speed}}{\text{Speed of Sound}} = \text{Mach Number}$$



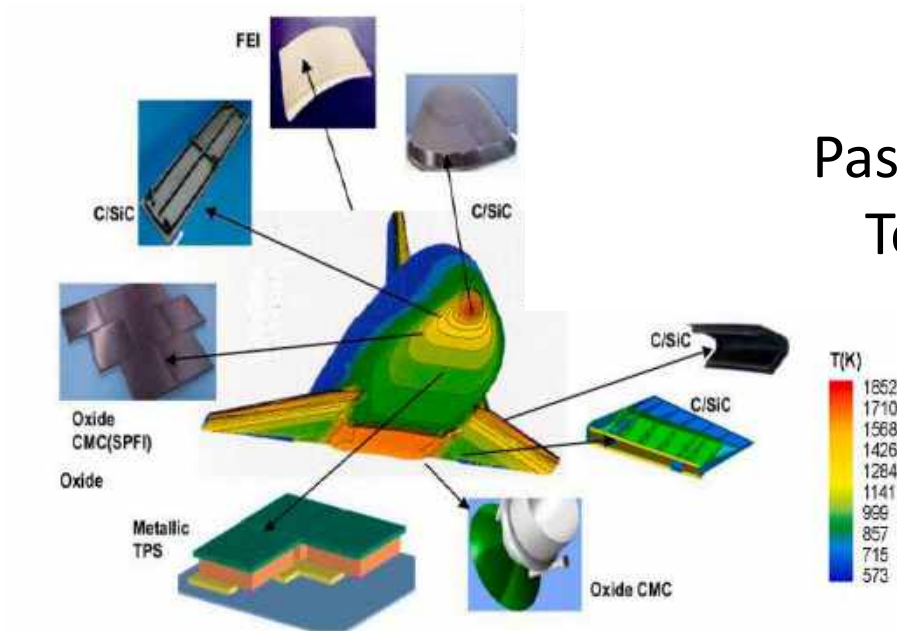
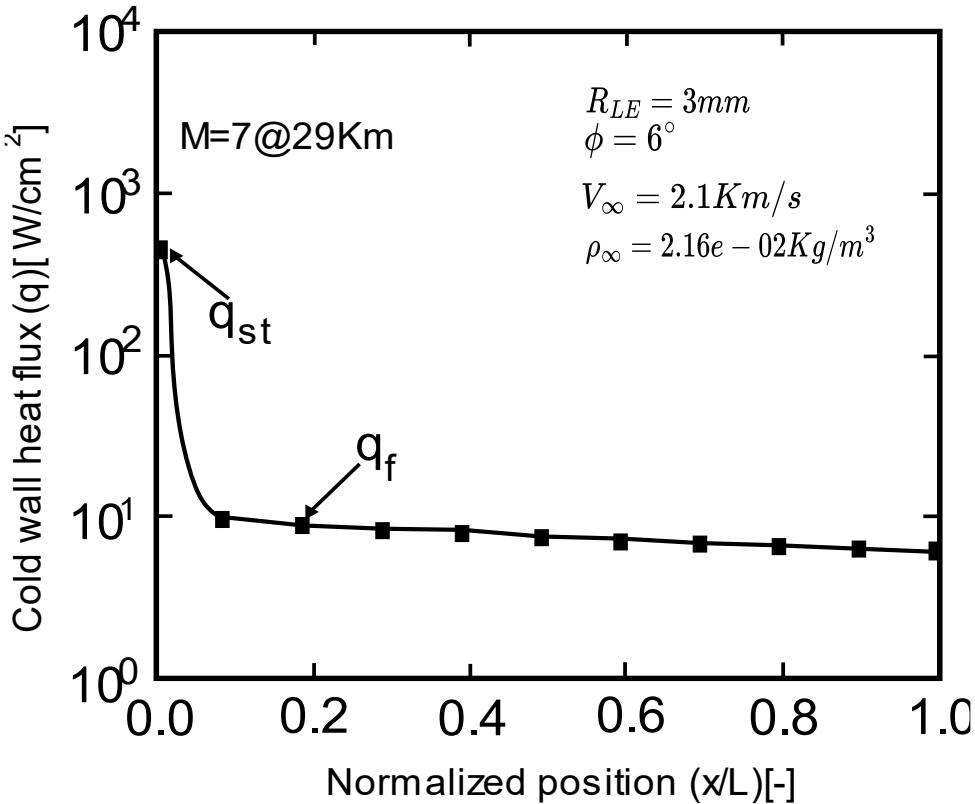
- Intensified flow phenomena
 - Viscous interaction
 - High temperature



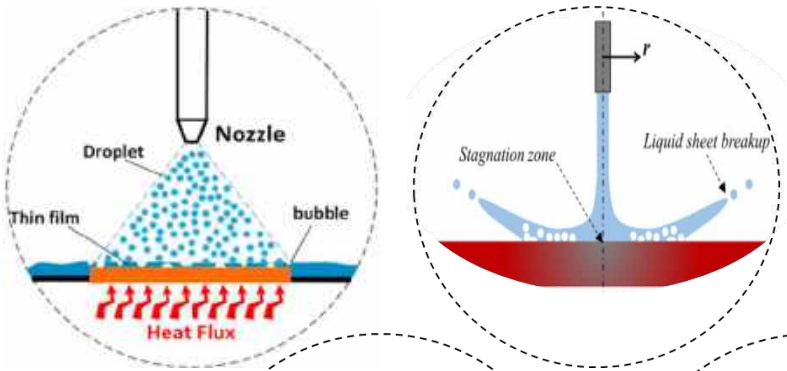
- \uparrow Aerodynamic heating $\rightarrow \downarrow$ L/D

$$T_o = T \left(1 + \frac{\gamma - 1}{2} M^2 \right)$$

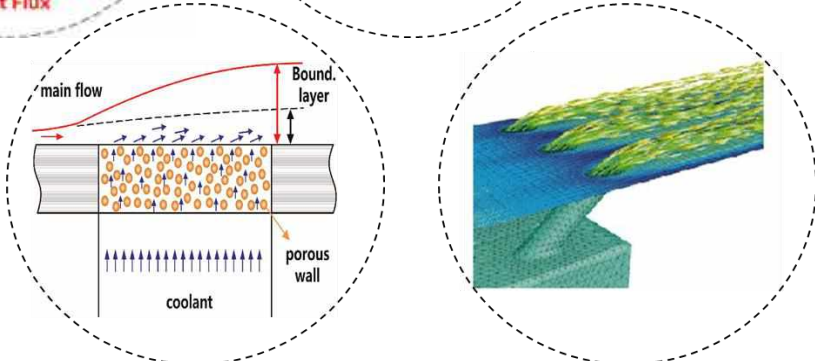
Aerodynamic heating on LE



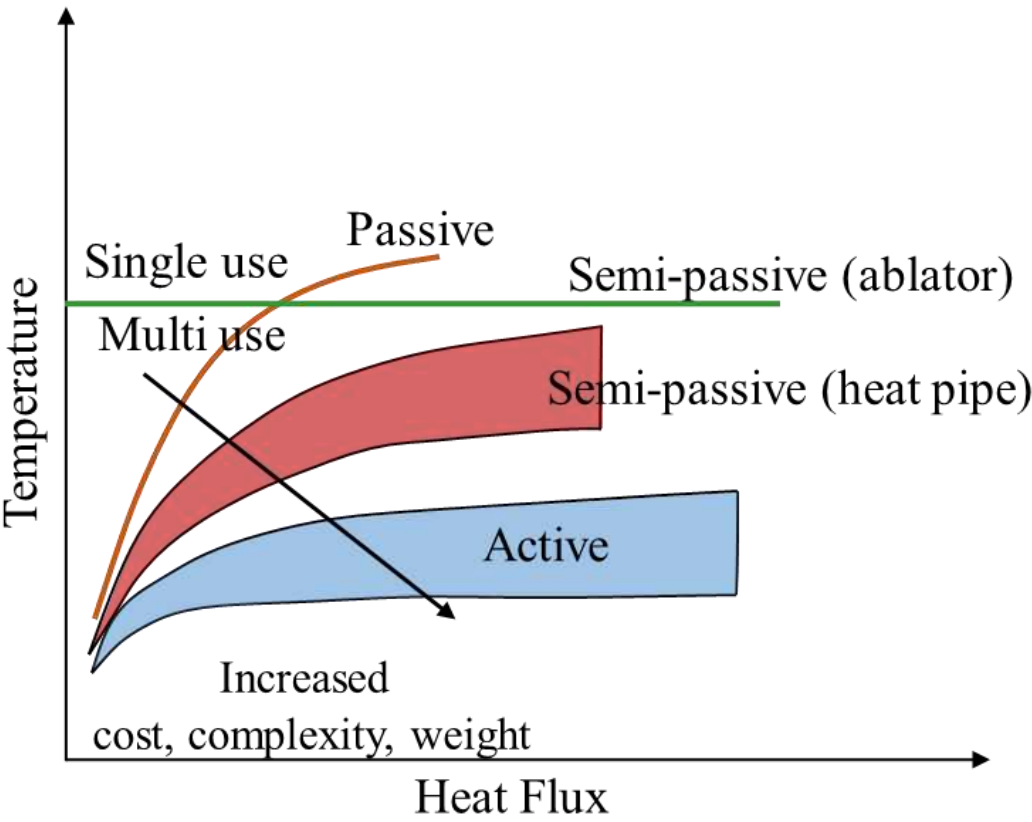
Passive Cooling Techniques



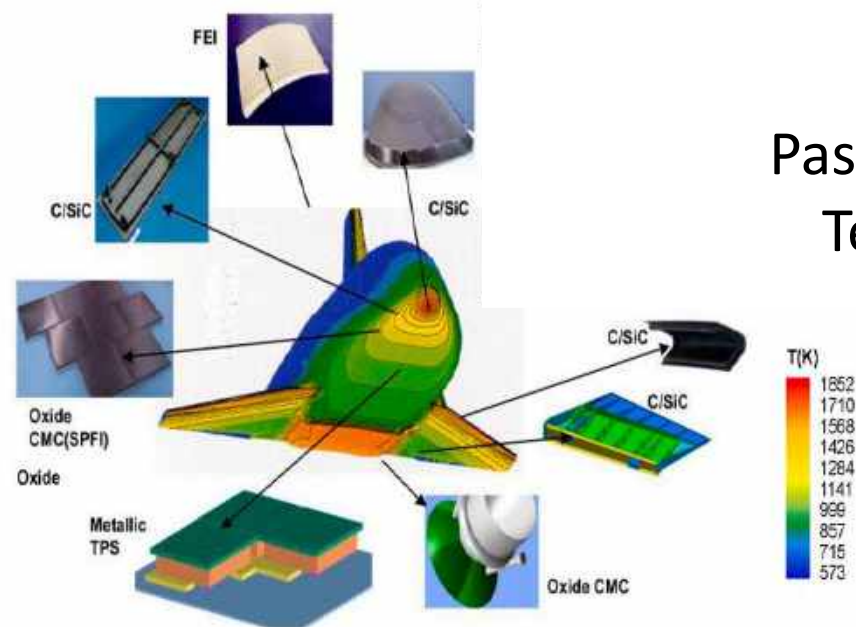
Active Cooling Techniques



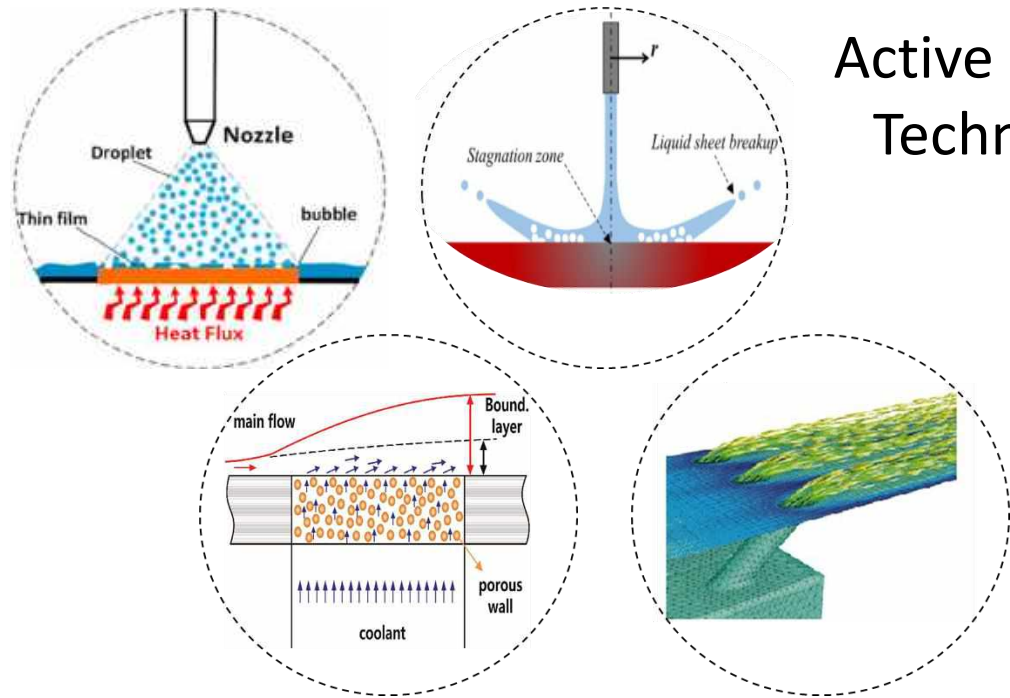
Aerodynamic heating on LE



Passive Cooling Techniques

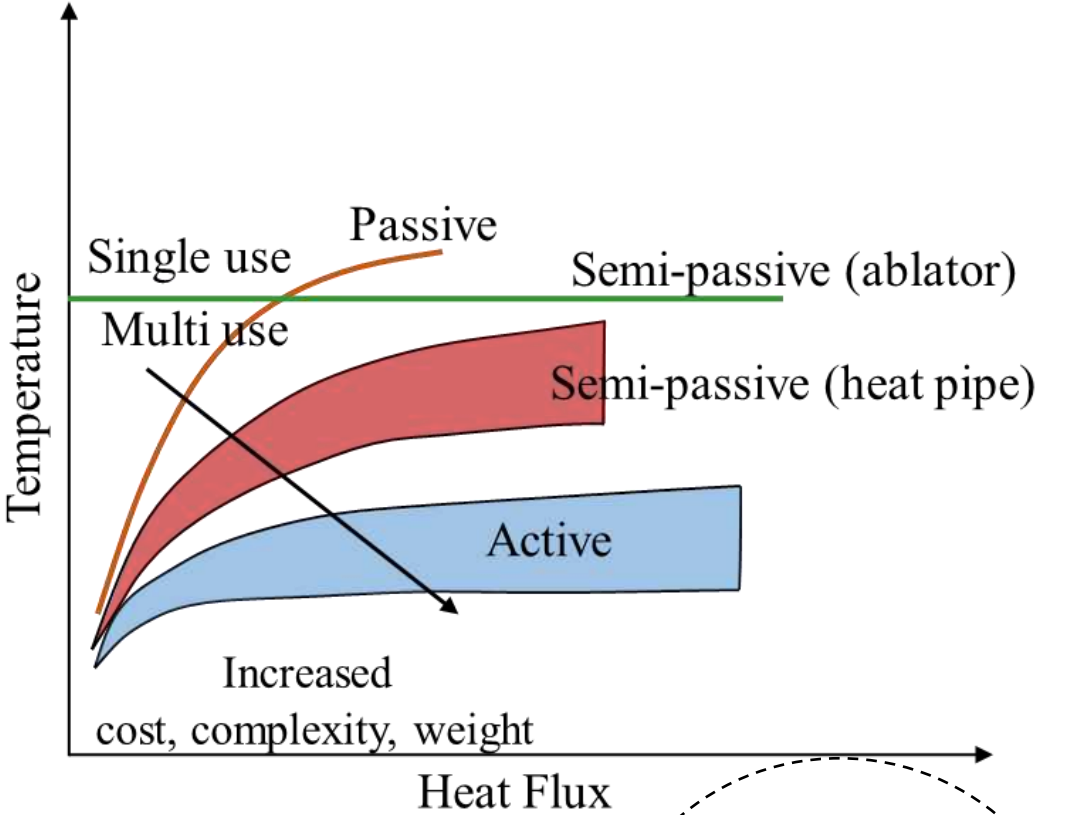


Active Cooling Techniques

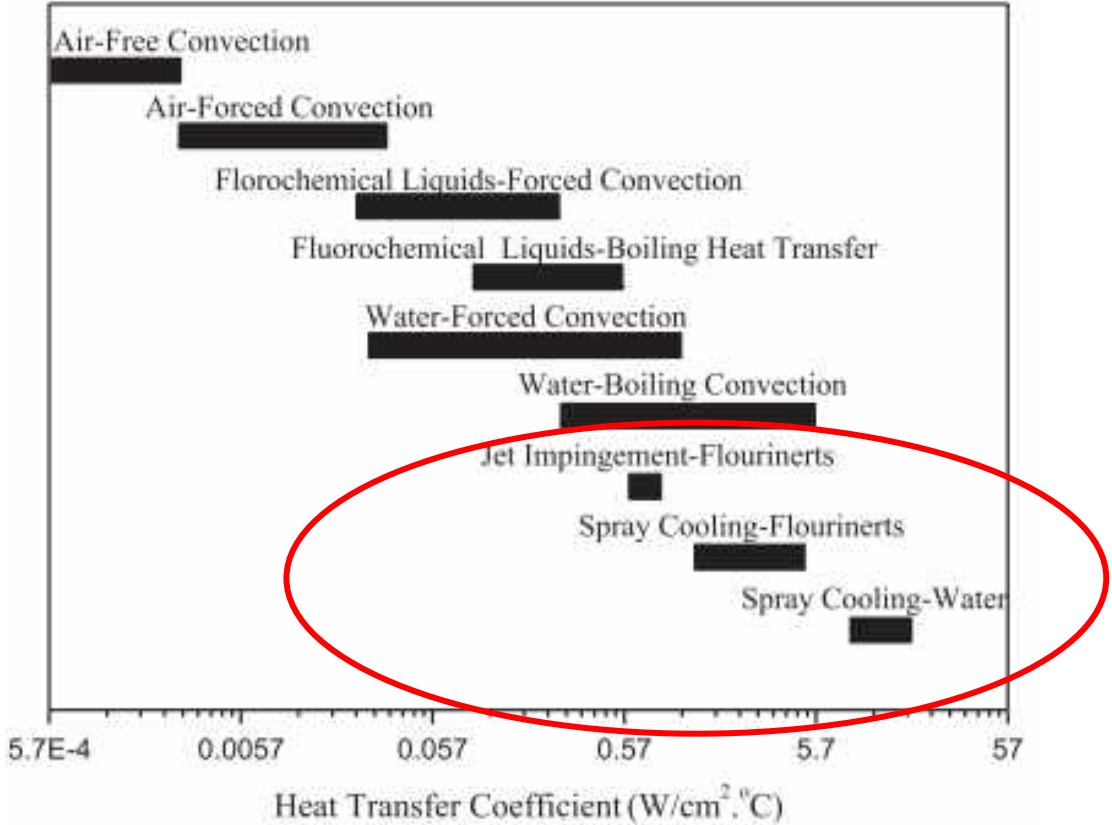
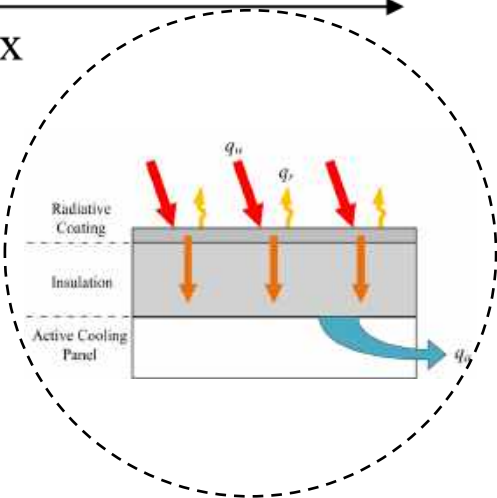


- Sustainable solution
- Effective handling of high T and q
- Active-Passive combination

Aerodynamic heating on LE



Hybrid Method



Challenges:

- Confined LE (1-3 mm radii)
- Extreme thermal loads
- Insufficient Passive TPS

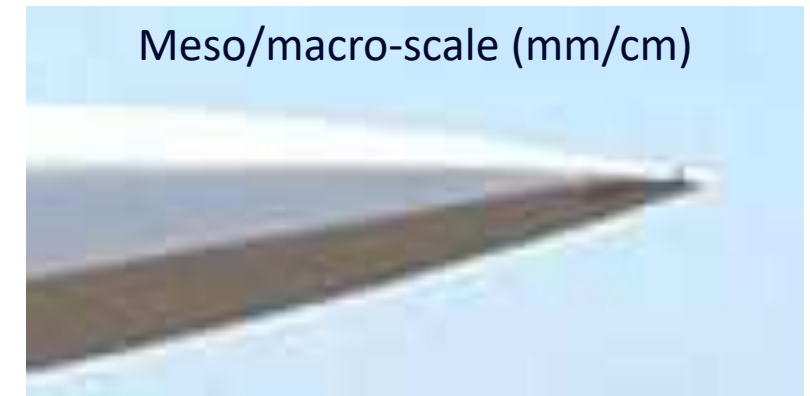
MSc Research Objective & Methodology

Motivation: Make hypersonic flights feasible

- Maintain aerodynamic efficiency
- Effectively manage extreme thermal loads

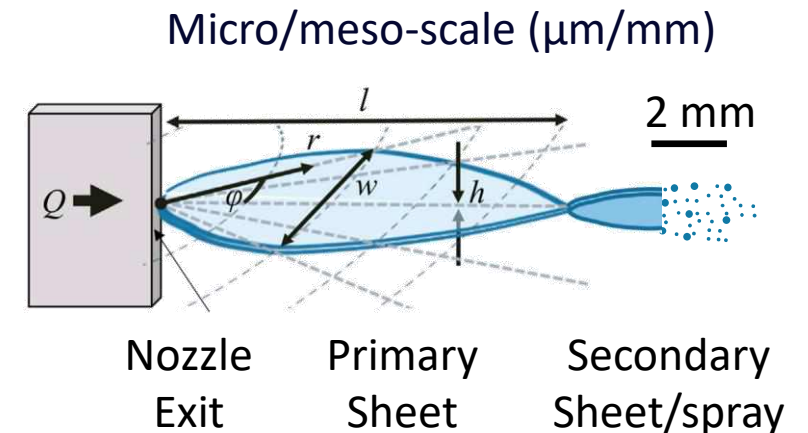


Objective: Develop an internal active cooling system for sharp and slender leading edges



Methods: Parametrically design and develop a microfluidic device for liquid sheet/spray cooling to characterize the:

- Dynamics of liquid sheets
- Jet & spray breakup





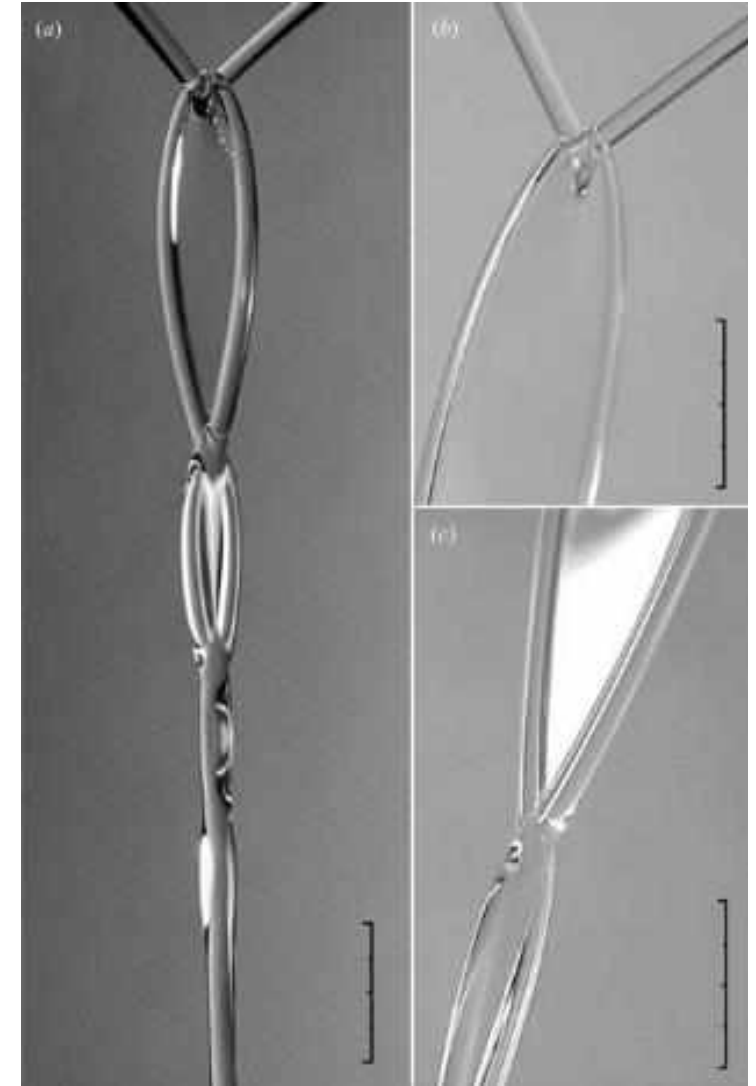
Presentation Outline

1. Introduction
- 2. Liquid sheets**
3. Experimental Methods
4. Numerical Methods
5. Results
6. Summary and Conclusions



Liquid sheet formation

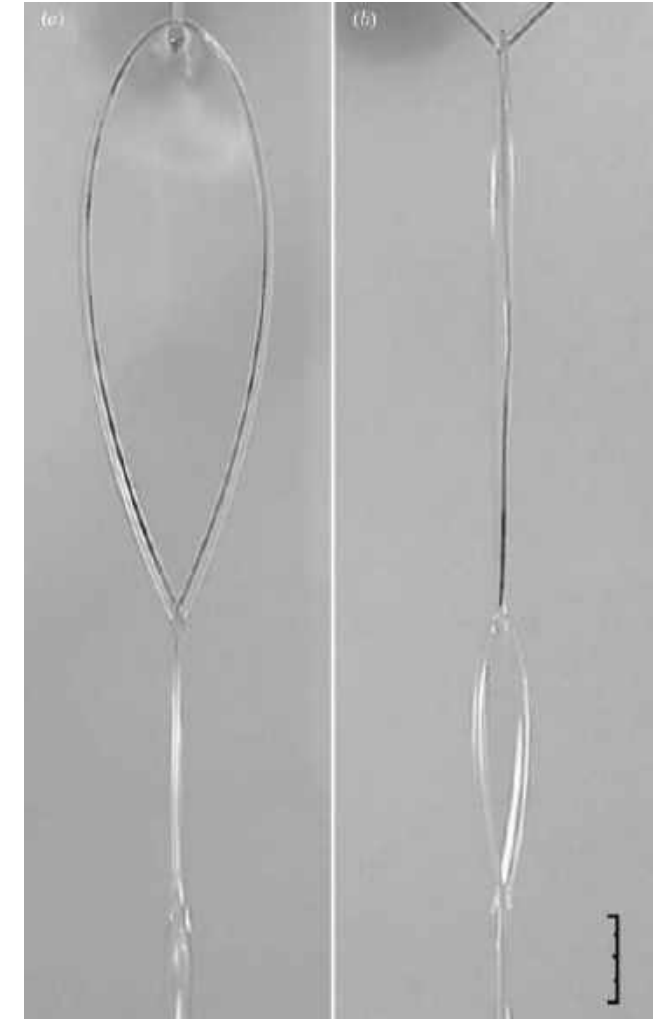
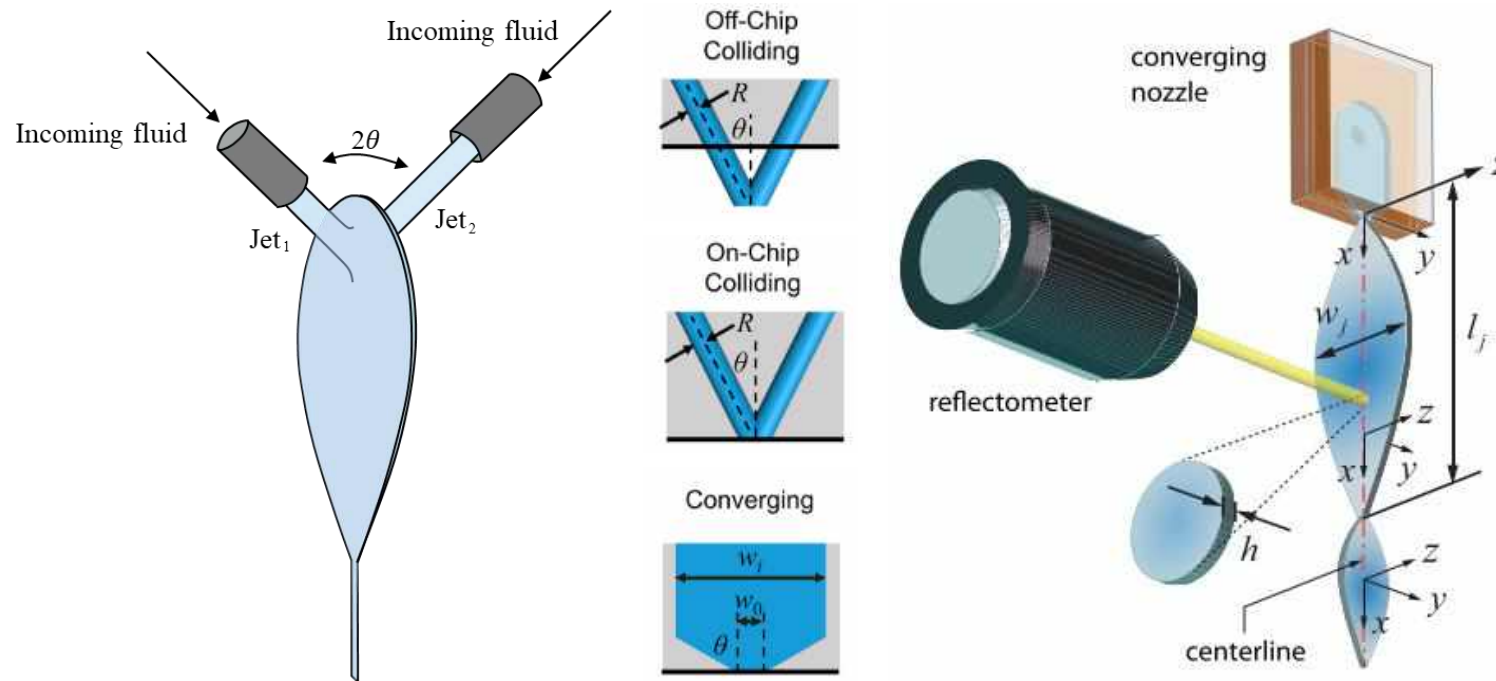
- Collision of two identical, high Re & coplanar jets at an oblique angle
- Dynamics dominated by surface tension & inertia
- Liquid sheet generation perpendicular to the plane of incidence
- Leaf-shaped links, formed in mutually orthogonal planes



A fluid chain resulting from the collision of a pair of identical laminar jets of a glycerol–water solution.
Scale bar: 1cm

Liquid sheet generation

- Impinging jets approach
 - Instabilities due to jet collision
 - Higher sensitivity to external perturbations
 - Jet misalignment
- In-chip flow-channels approach

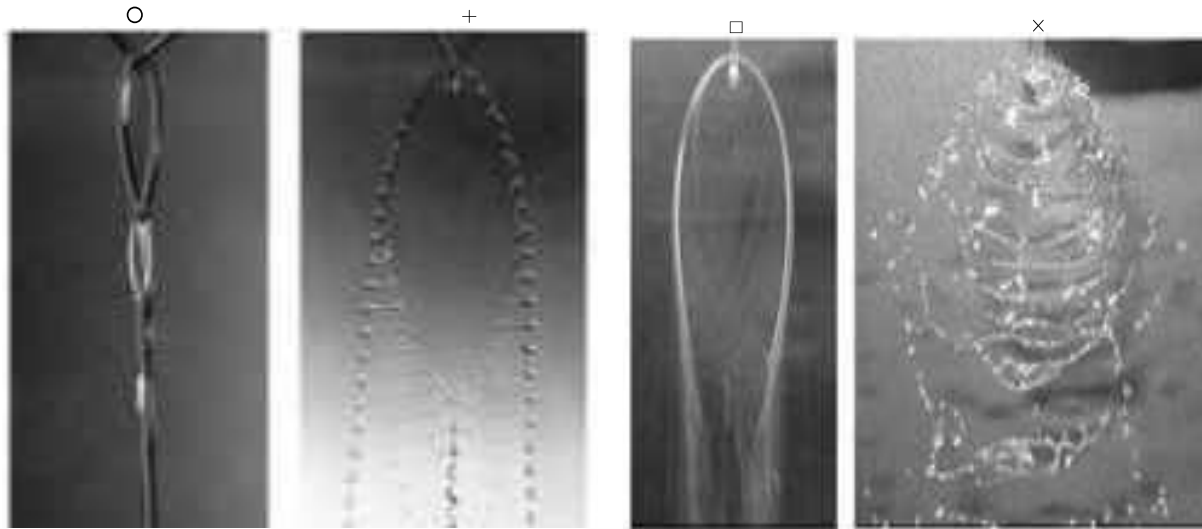


Front & side views of the fluid chain resulting from the collision of a pair of identical laminar jets¹⁰

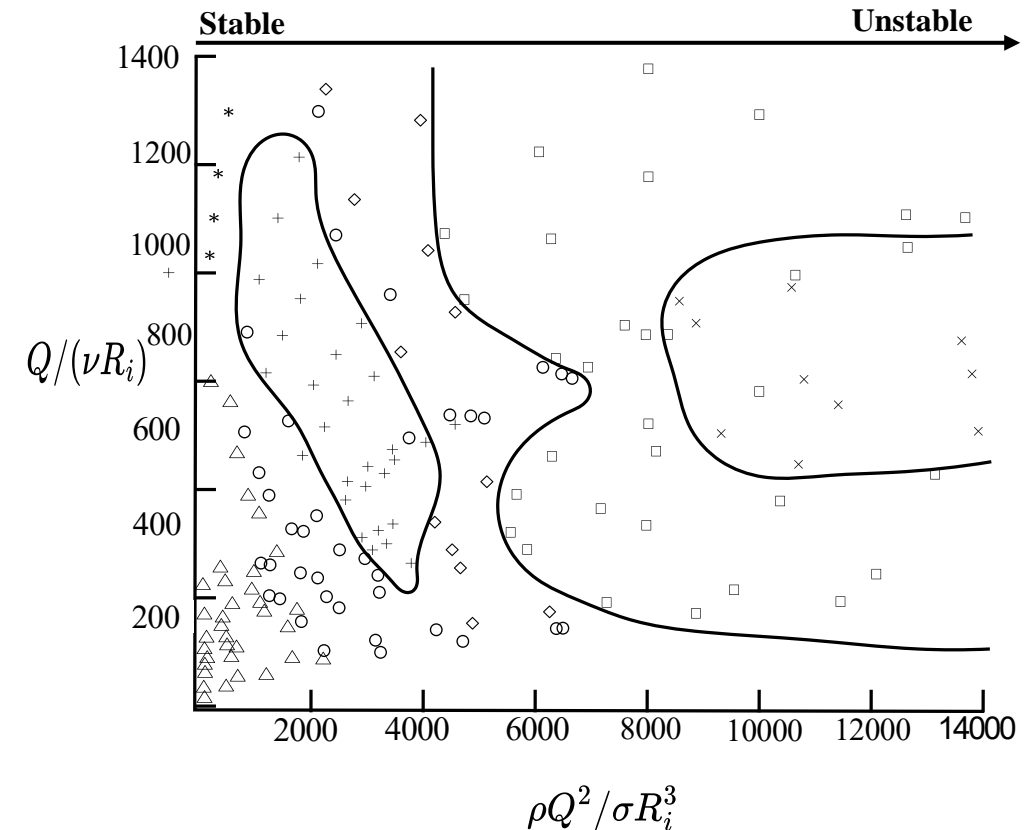
Liquid sheet morphology

- Dynamics described by Reynolds (Re) & Weber (We) numbers

$$\text{Re} = \frac{Q}{\nu R_j} \quad \& \quad \text{We} = \frac{\rho Q^2}{\sigma R_j^3}$$



Symbol	Behaviour
\triangle	Oscillating streams
\star	Sheets with disintegrating rims
\circ	Fluid chains
$+$	Fish-bones
\diamond	Spluttering chains
\square	Disintegrating sheets
\times	Violent flapping



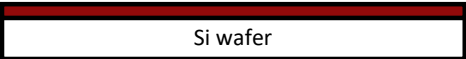


Presentation Outline

1. Introduction
2. Liquid sheets
- 3. Experimental Methods**
4. Numerical Methods
5. Results
6. Summary and Conclusions

Nozzle chips fabrication

1) Spin coat photoresist



2) Expose mask geometry and develop



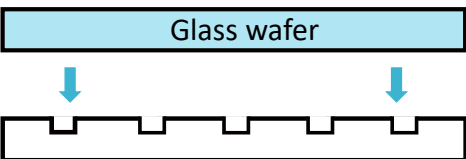
3) Deep Reactive Ion Etching



4) Strip photoresist



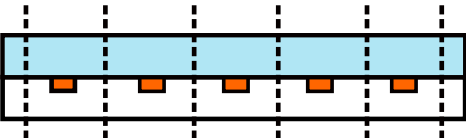
5) Wafer alignment & Anodic bonding



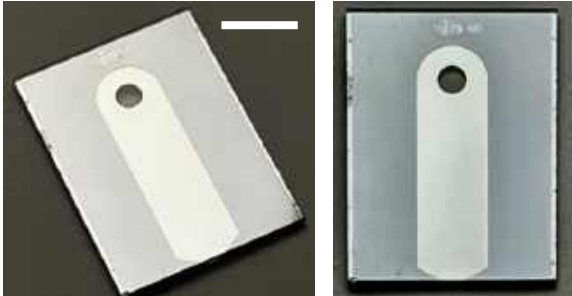
6) Channel filling with wax



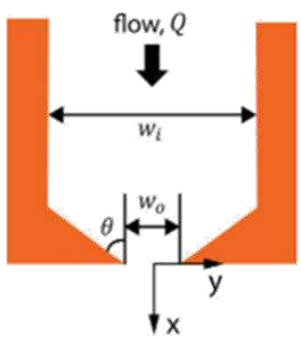
7) Dicing



8) Polishing

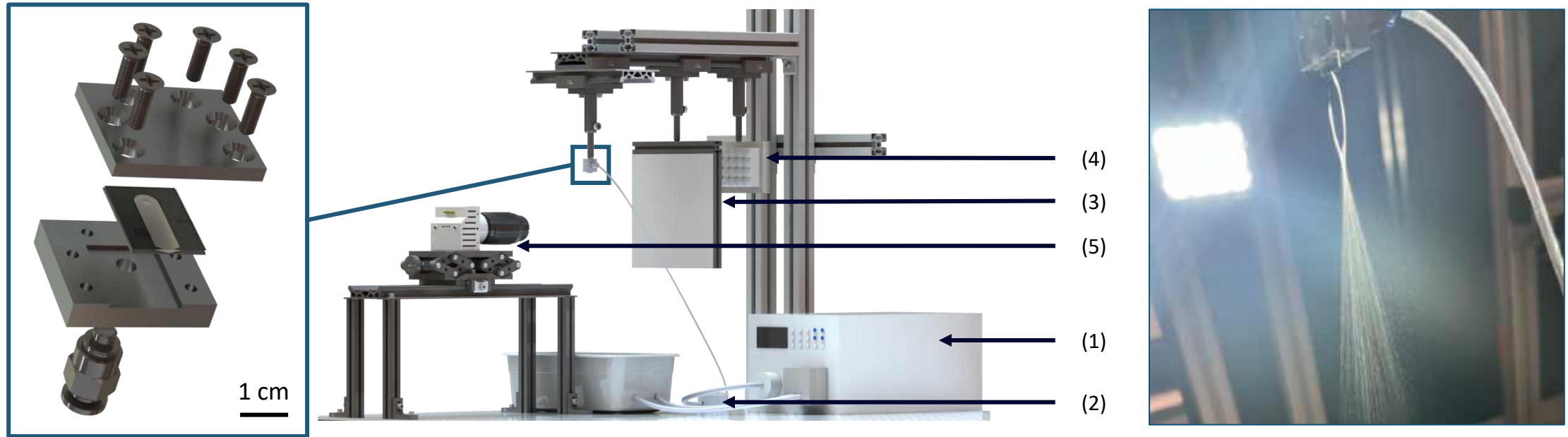


Scale bar: 5 mm



Nozzle thickness	t	μm	50-150
Outlet width	w_o	μm	250-1000
Nozzle angle	ϑ	deg	40-80
Flow rate	Q	ml/min	20-100

Shadowgraph Imaging setup



- HPLC dosing unit (1) with external pulse dampener (2) for DI water flow
- Backlight-diffused illumination (3 & 4) for shadowgraph imaging (5)
- 100 kHz framerate with 8.93 μs exposure time
- 70 $\mu\text{m}/\text{px}$ optical magnification

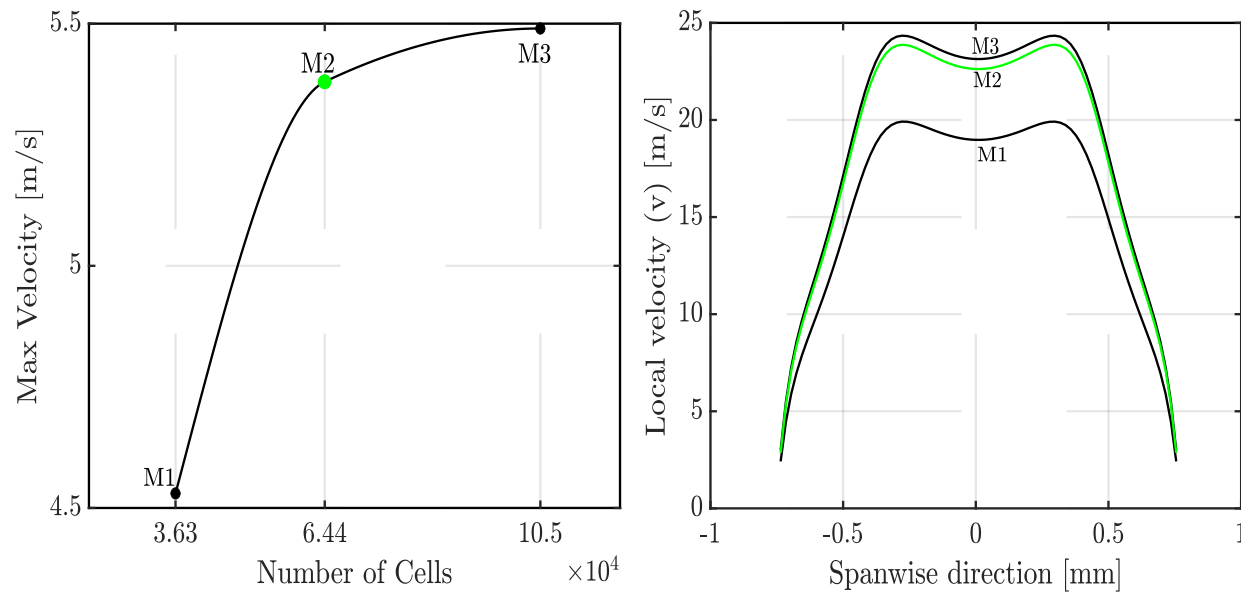
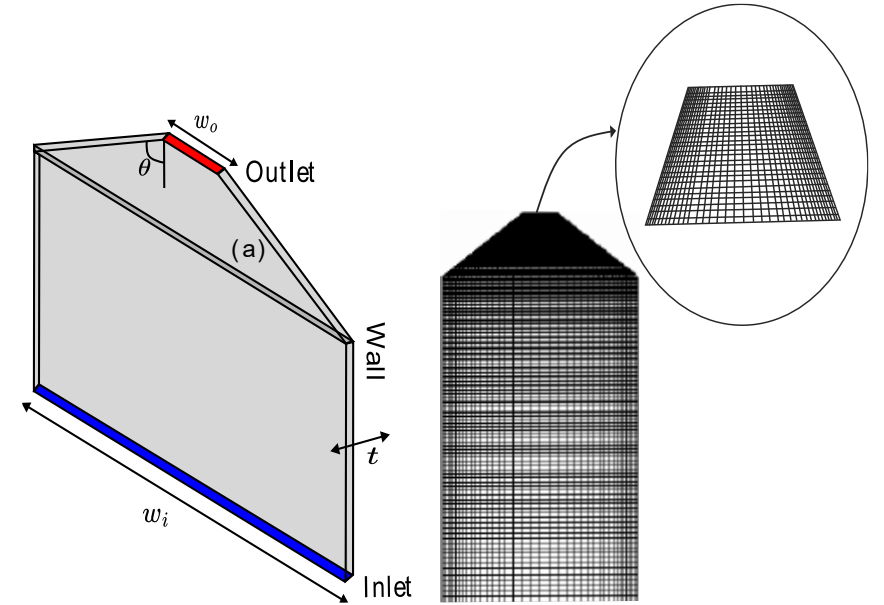


Presentation Outline

1. Introduction
2. Liquid sheets
3. Experimental Methods
- 4. Numerical Methods**
5. Results
6. Summary and Conclusions

Numerical simulation configuration

- ANSYS Fluent 2022 R1
- Grid Independence study
 - Longitudinal velocity profile evaluation
 - Outlet width - $w_o = 900 \mu\text{m}$
 - Inlet width - $w_i = 4950 \mu\text{m}$
 - Nozzle thickness- $t = 60 \mu\text{m}$
 - Nozzle angle - $\theta = 60^\circ$



Numerical setup and validation

- ANSYS Fluent 2022 R1
- Steady, incompressible and laminar solver
- Residuals criterion: 10^{-6}
- Validation with PIV measurements

Grid Convergence Index (GCI)

$$GCI = \frac{E_{mf}}{E_f} \left(\frac{r^p}{r^p - 1} \right) = \mathbf{1.135 < 5\%}$$

$$E_{mc} = \phi_m - \phi_c = 3.97$$

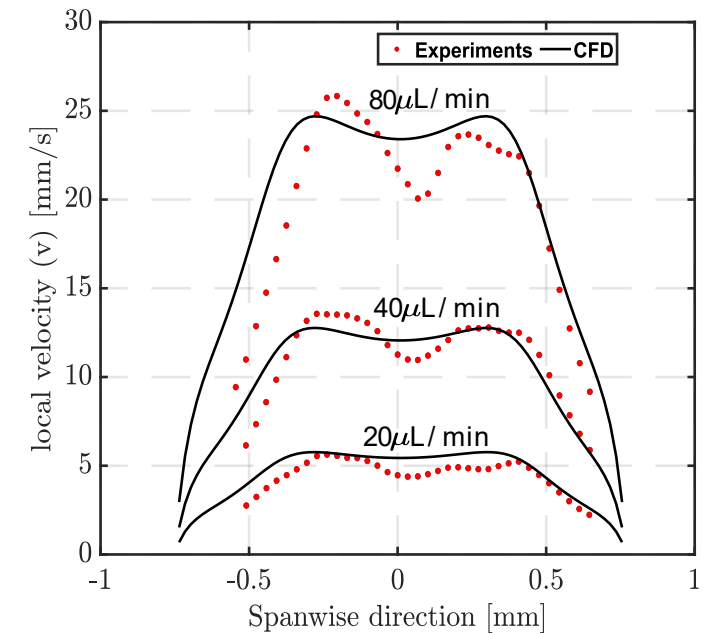
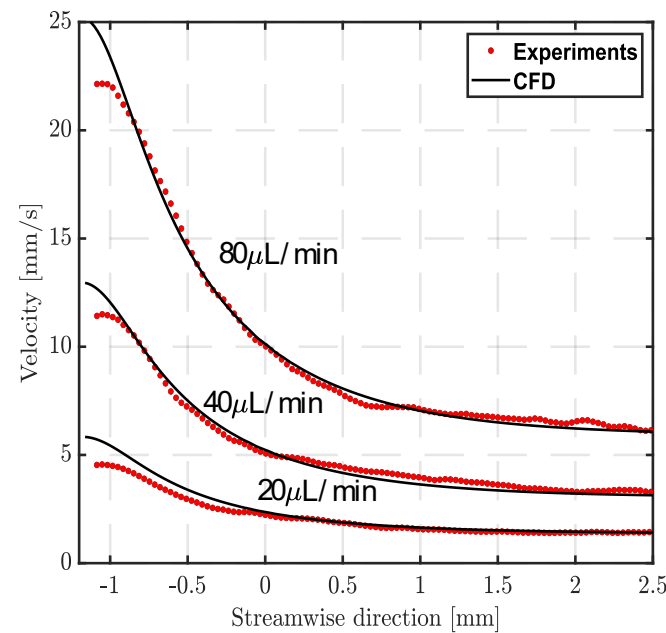
$$E_{mf} = \phi_f - \phi_m = 0.47$$

$$r = 1.6$$

r: Grid refinement ratio

$$p = \frac{\ln\left(\frac{E_{mc}}{E_{mf}}\right)}{\ln(r)} = 4.54$$

p: Order of convergence



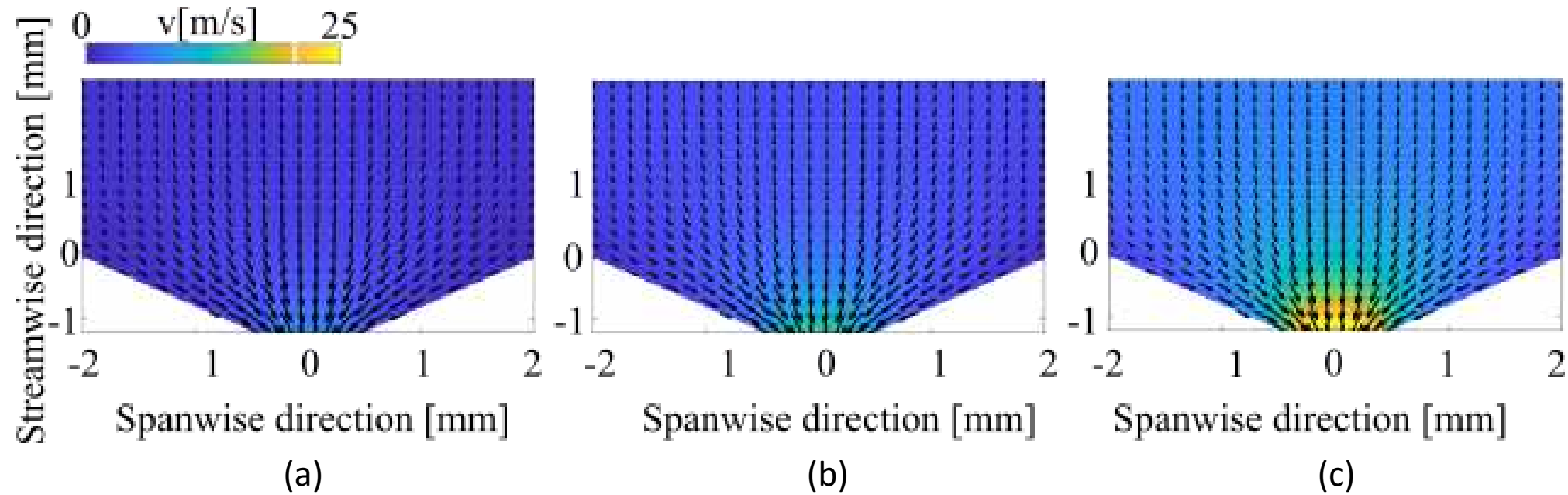


Presentation Outline

1. Introduction
2. Liquid sheets
3. Experimental Methods
4. Numerical Methods
- 5. Results**
6. Summary and Conclusions

Nozzle velocity field-CFD

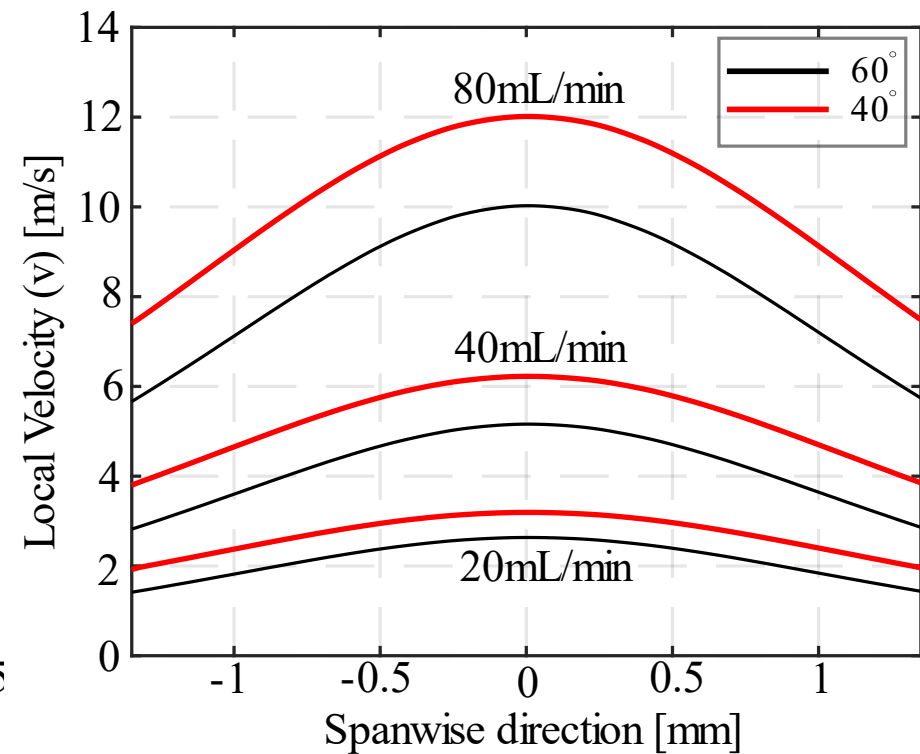
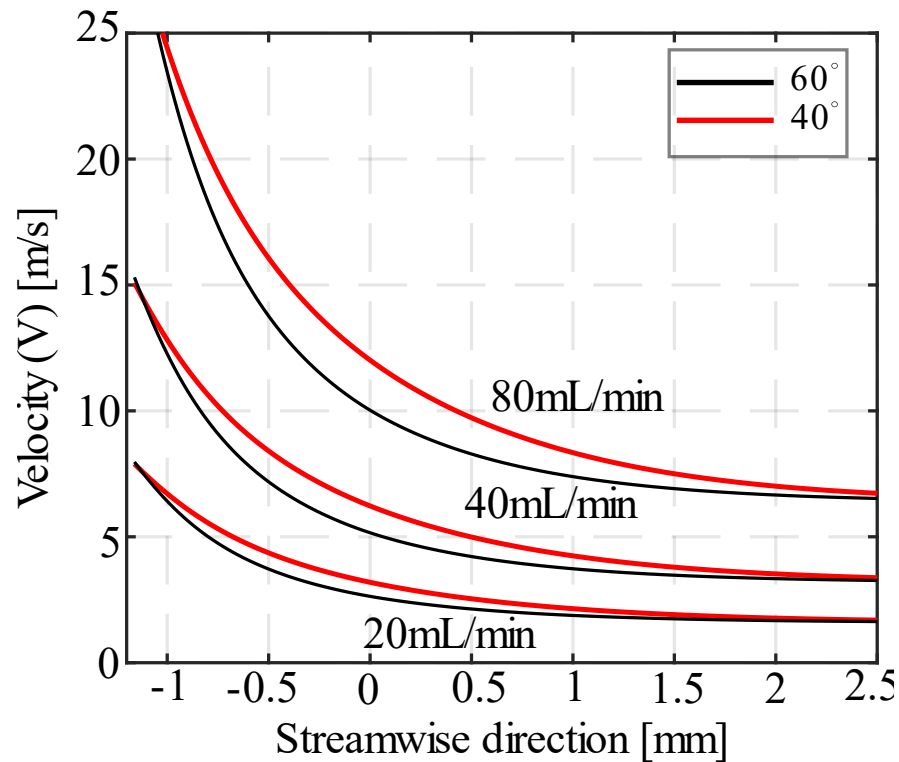
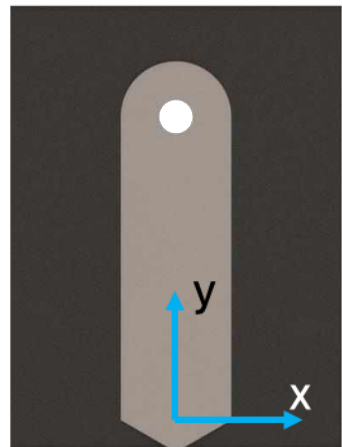
- Similar velocity field characteristics
- Laminar flow despite high Re
- No indications of flow non-uniformities & present disturbances



Comparison of longitudinal velocity contours and vector plots in the nozzle for varying flowrate (Q) of a) 20mL/min, b) 40mL/min, c) 80mL/min

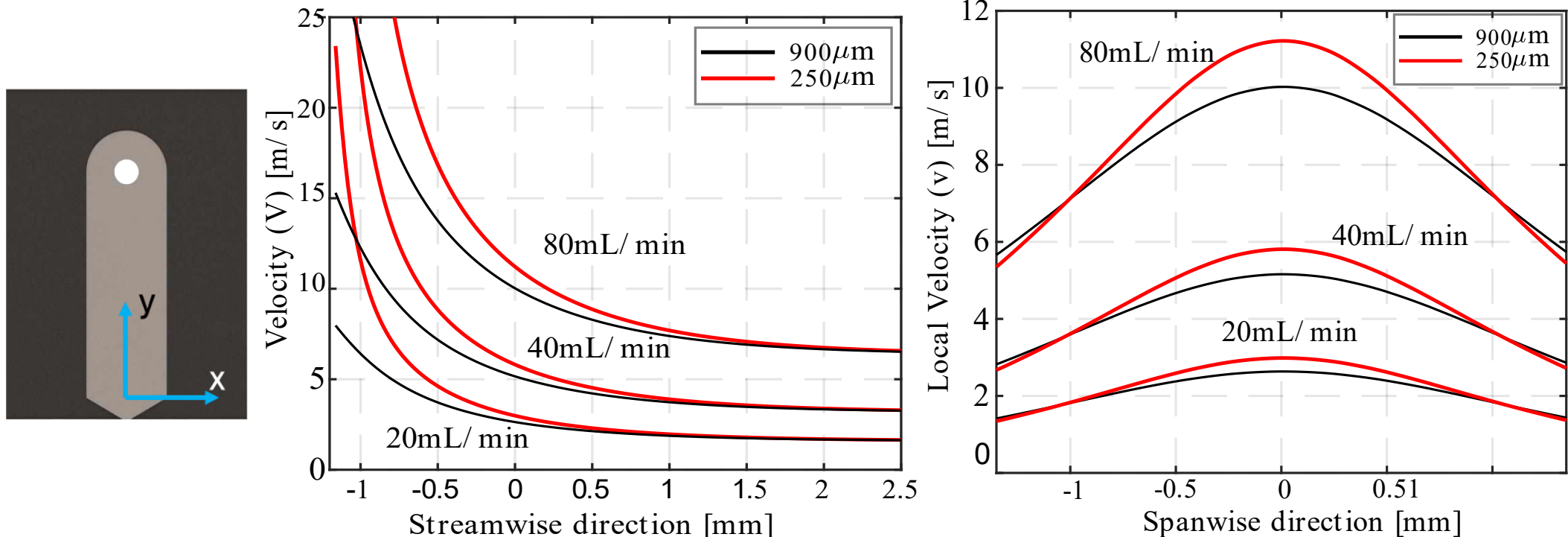
Nozzle velocity field - CFD

- Parametric investigation of nozzle angle θ variation effects
- Inversely analogous dependency between nozzle angle θ and the velocity field in the nozzle
- Exit velocity dependent only on outlet dimensions



Nozzle velocity field - CFD

- Parametric investigation of outlet width w_o variation effects
- Inversely analogous dependency between outlet width w_o and the velocity field
- Augmented exit velocity due to smaller outlet cross-sectional area

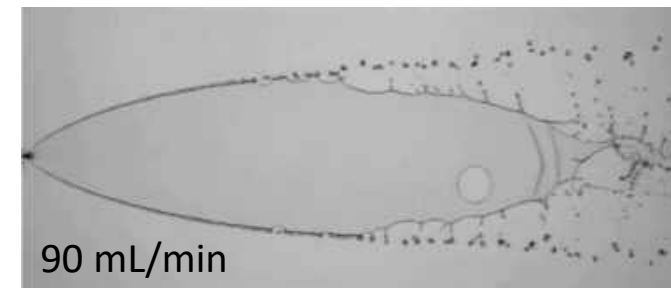
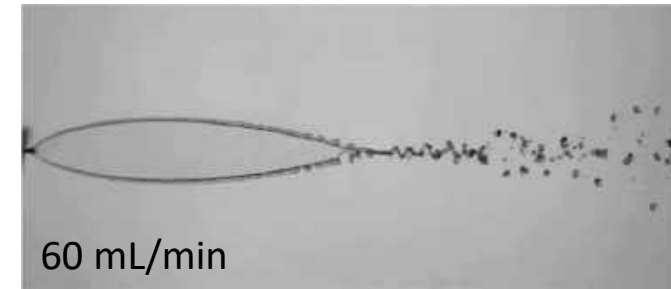
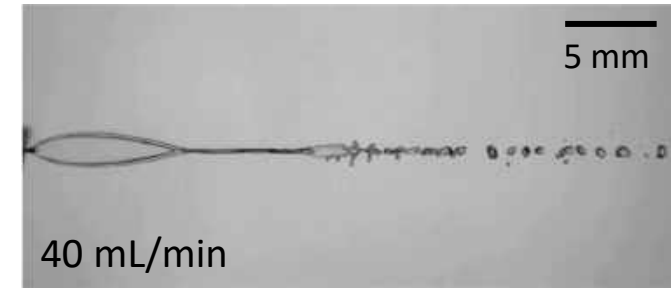
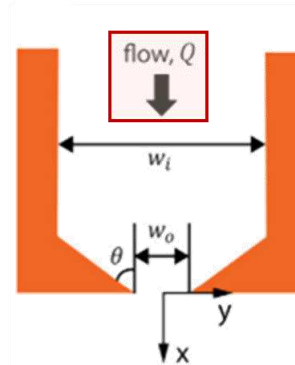




Effect of Q-variation on sheet dynamics

- Nozzle geometry
 - $w_o = 750 \mu\text{m}$, $\theta = 40^\circ$ and $t = 100 \mu\text{m}$
- Video playback speed – 1650 times slower
- Gradual rim thickness change
- Increasing length and width
- Decreasing number of links
- Rim breakup before the link's apex
- Literature quantification of flowrate effects on liquid sheet size

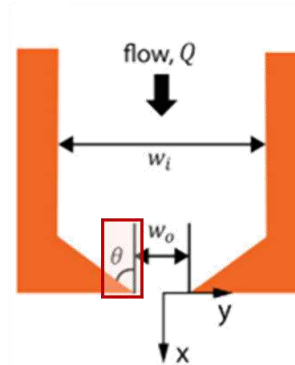
$$\{l_s, w_s\}(Q) \sim We \cdot Ca^m$$



Effect of θ -variation on sheet dynamics

- Nozzle geometry and flow conditions
 - $w_o = 750 \mu\text{m}$, $Q=30 \text{ mL/min}$ and $t = 100 \mu\text{m}$
- Video playback speed – 1100 times slower
- Length and width fluctuation
- Max sheet size at $\theta \approx 55^\circ$
- Rim instability propagation with $\theta \uparrow$
- Drop shedding from rims at $\theta \geq 70^\circ$
- Literature quantification of nozzle angle effects on liquid sheet size

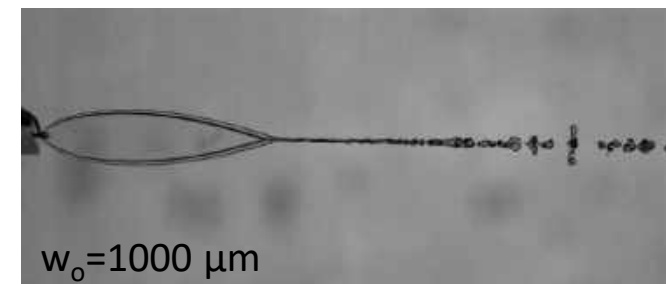
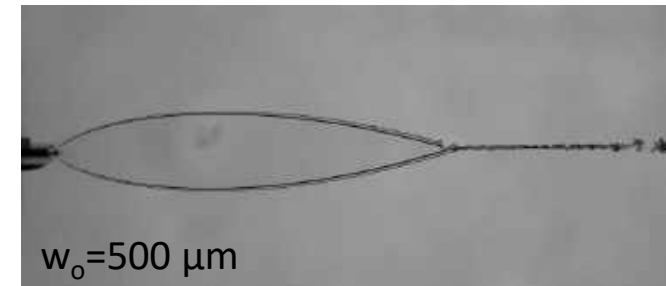
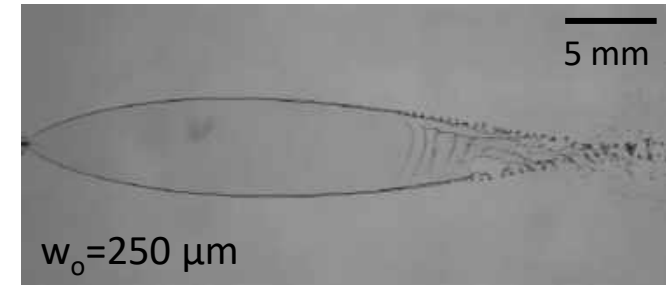
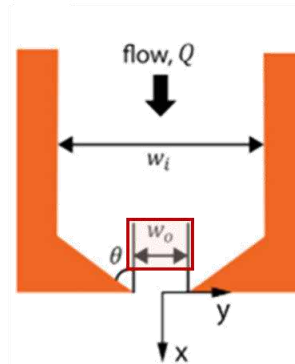
$$\{l_s, w_s\}(\theta) \sim [1 + \cot(0.67\theta)]^{-n}$$



Effect of w_o -variation on sheet dynamics

- Nozzle geometry and flow conditions
 - $\theta = 60^\circ$, $Q=60$ mL/min and $t = 150$ μm
- Video playback speed – 1100 times slower
- A_{ex} increase and V_{ex} decrease
- Length and width decrease
- Instability damping & Breakup delay
- Shift from spray to jet breakup
- Literature quantification of outlet width effects on liquid sheet size

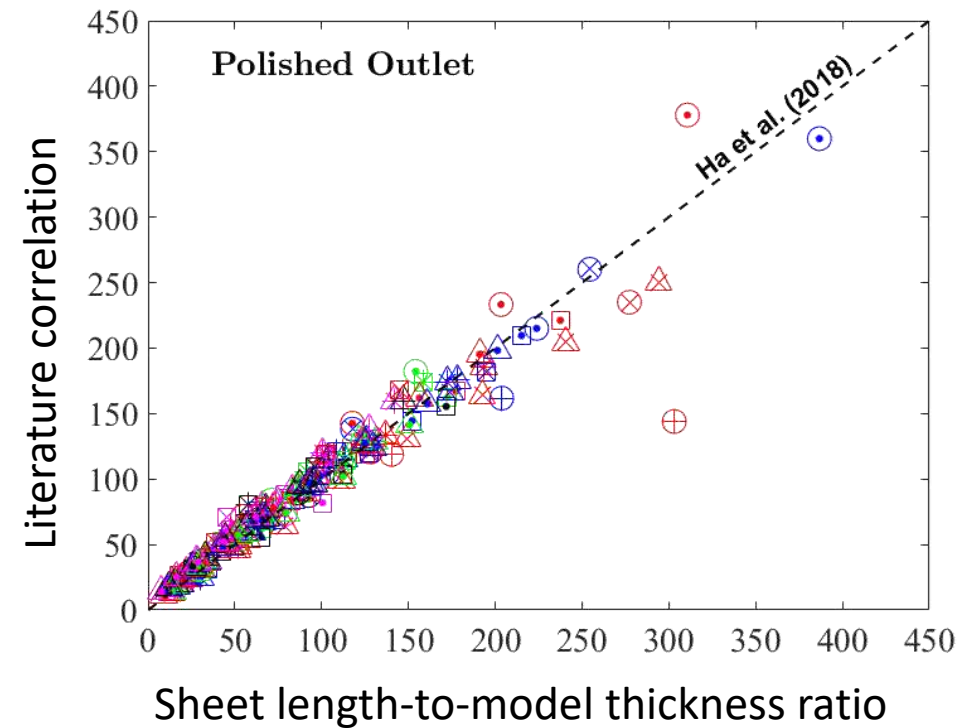
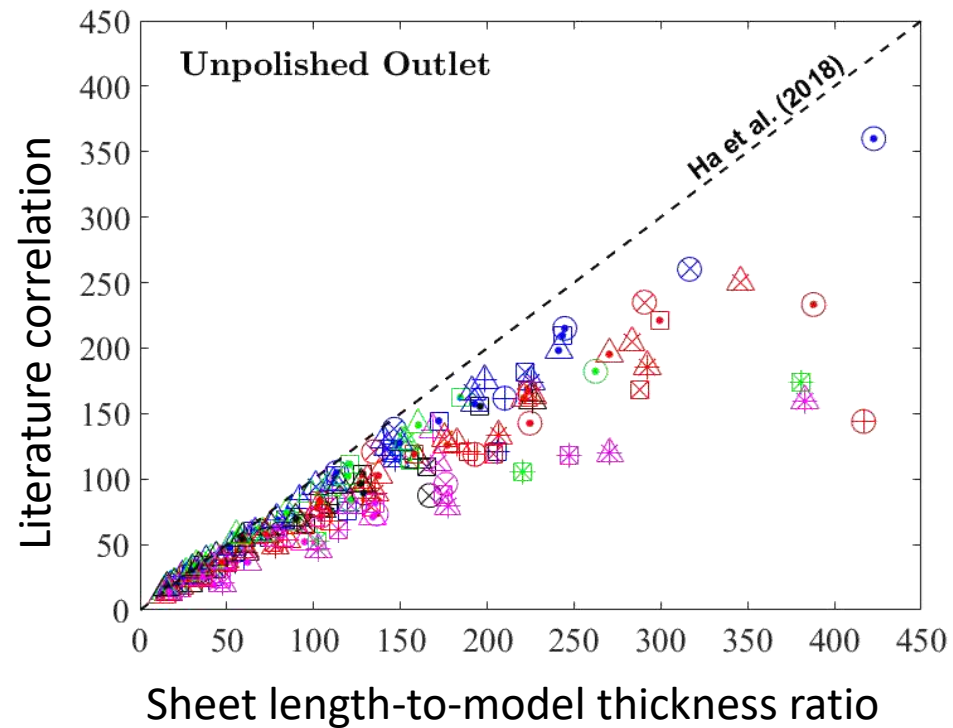
$$\{l_s, w_s\}(w_o) \sim (1 + 1.5\alpha^2)^{-n}$$





Outlet polishing effects on sheet length

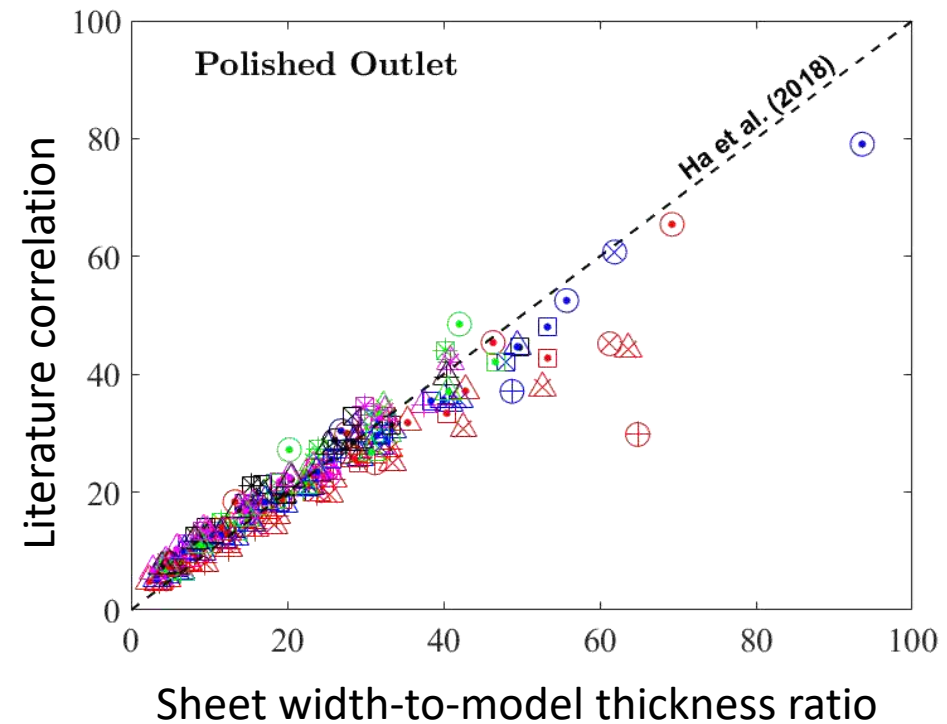
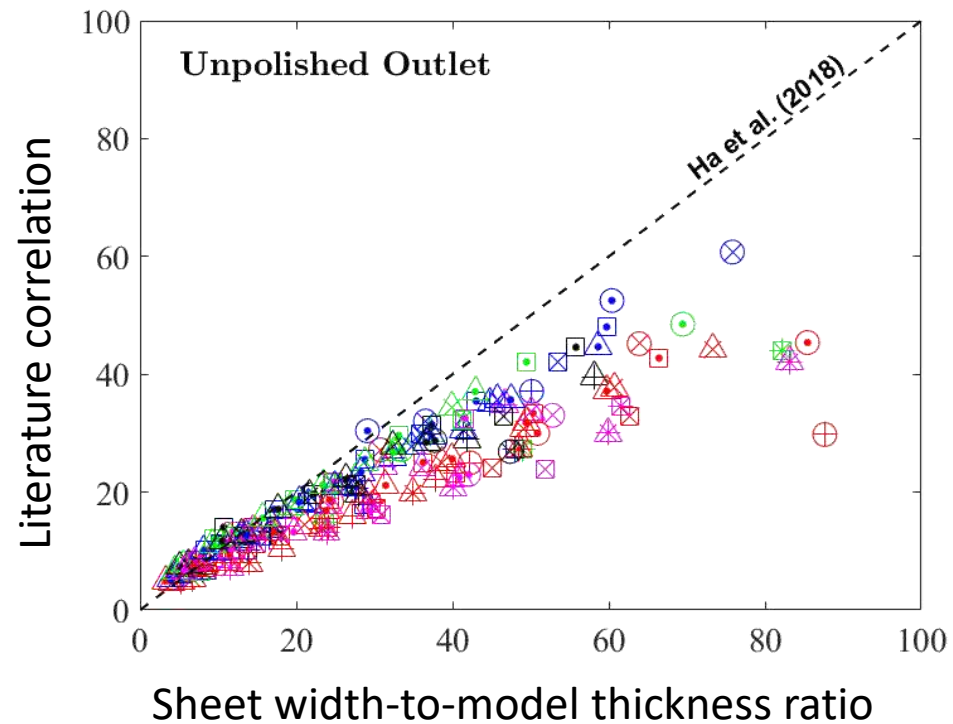
$$l_s/t = 0.23We \cdot Ca^{-0.1}(1+1.5\alpha^2)^{-0.5}[1+\cot(0.67\theta)]^{-0.5}$$





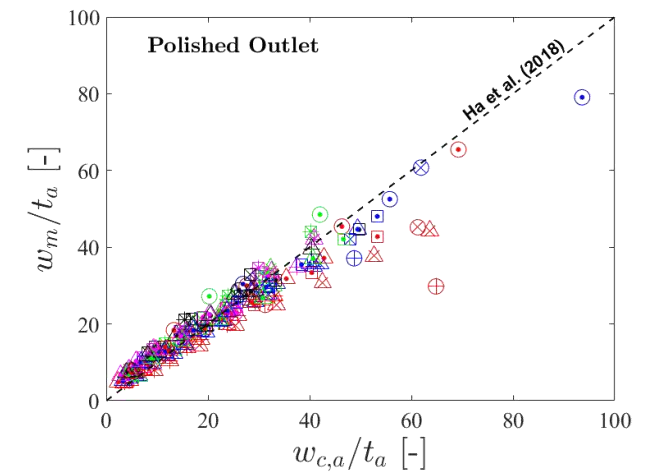
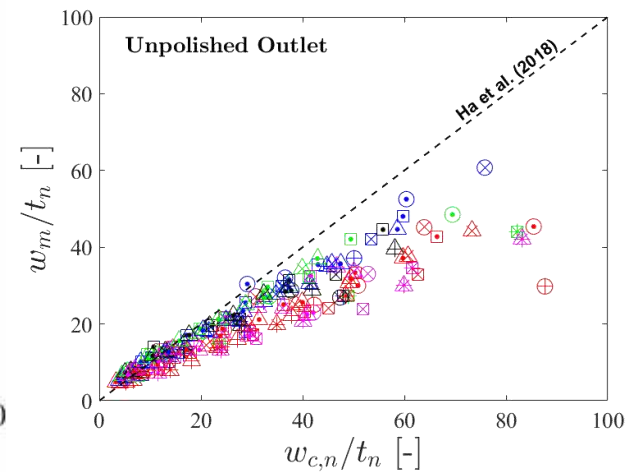
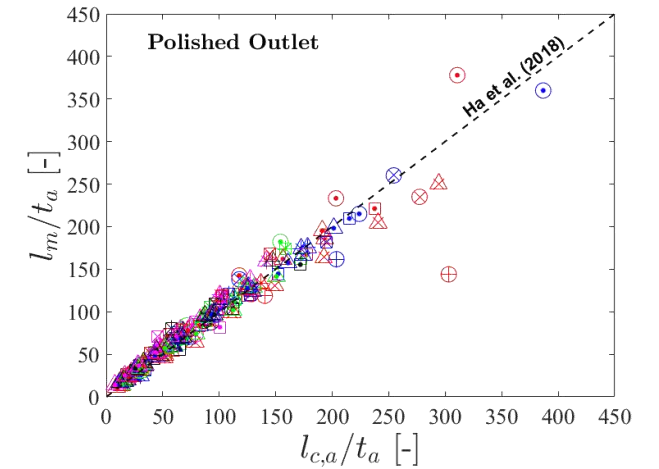
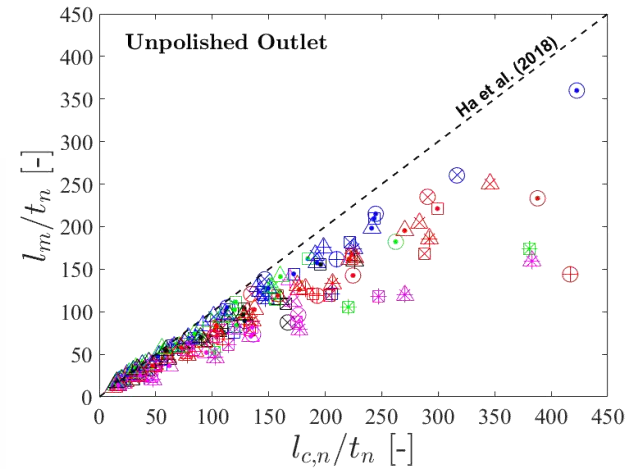
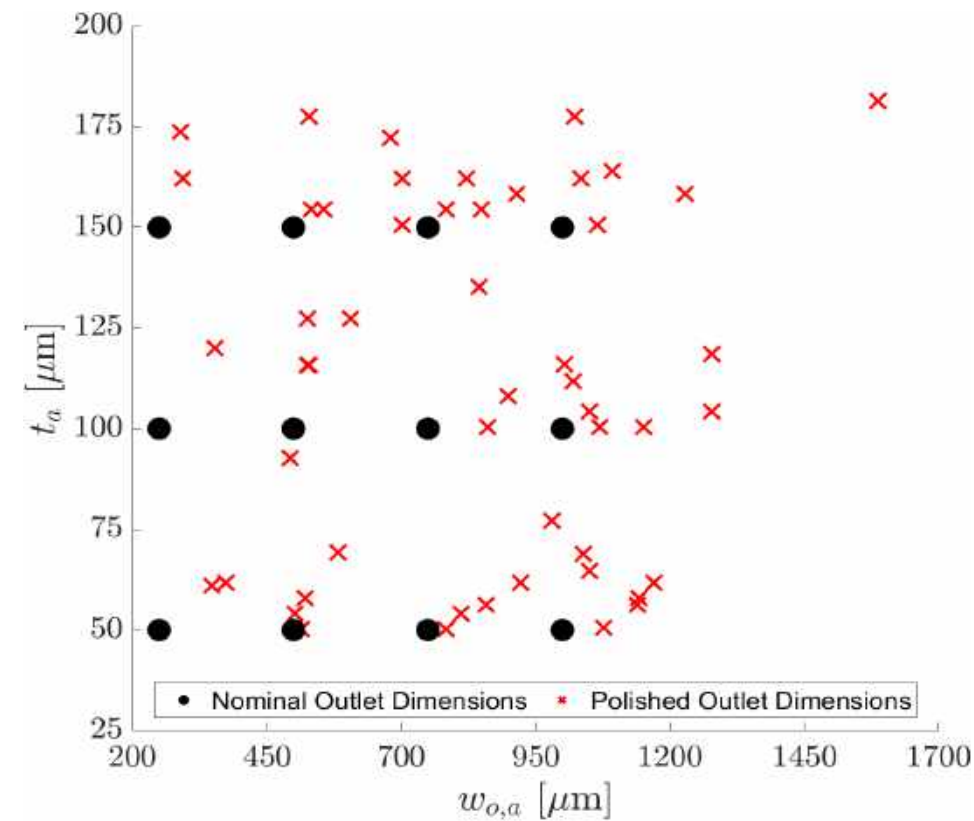
Outlet polishing effects on sheet width

$$w_s/t = 0.074We \cdot Ca^{-0.2}(1+1.5\alpha^2)^{-1}[1+\cot(0.67\theta)]^{-1}$$



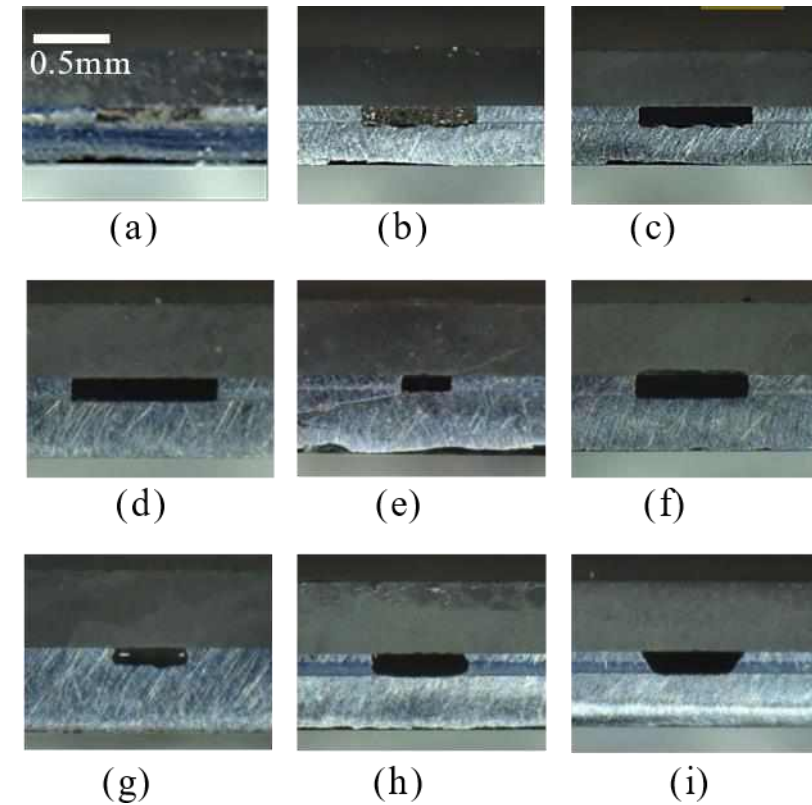
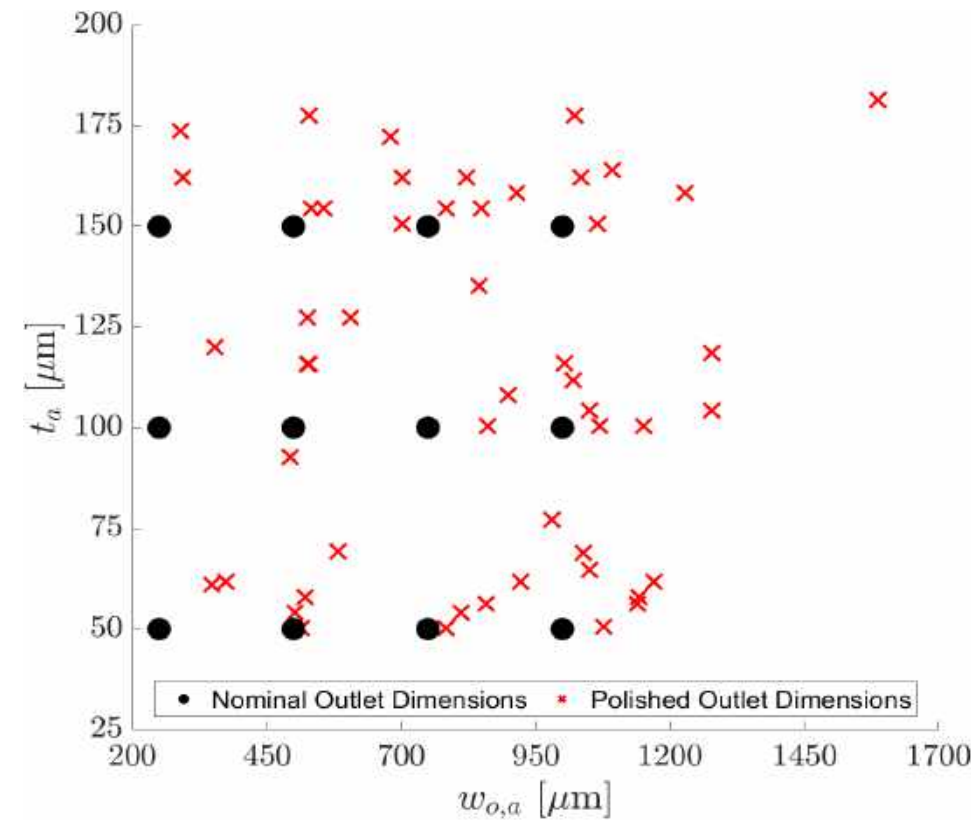
Design point shift due to polishing

- Outlet dimensions increase



Polishing-exposed fabrication flaws

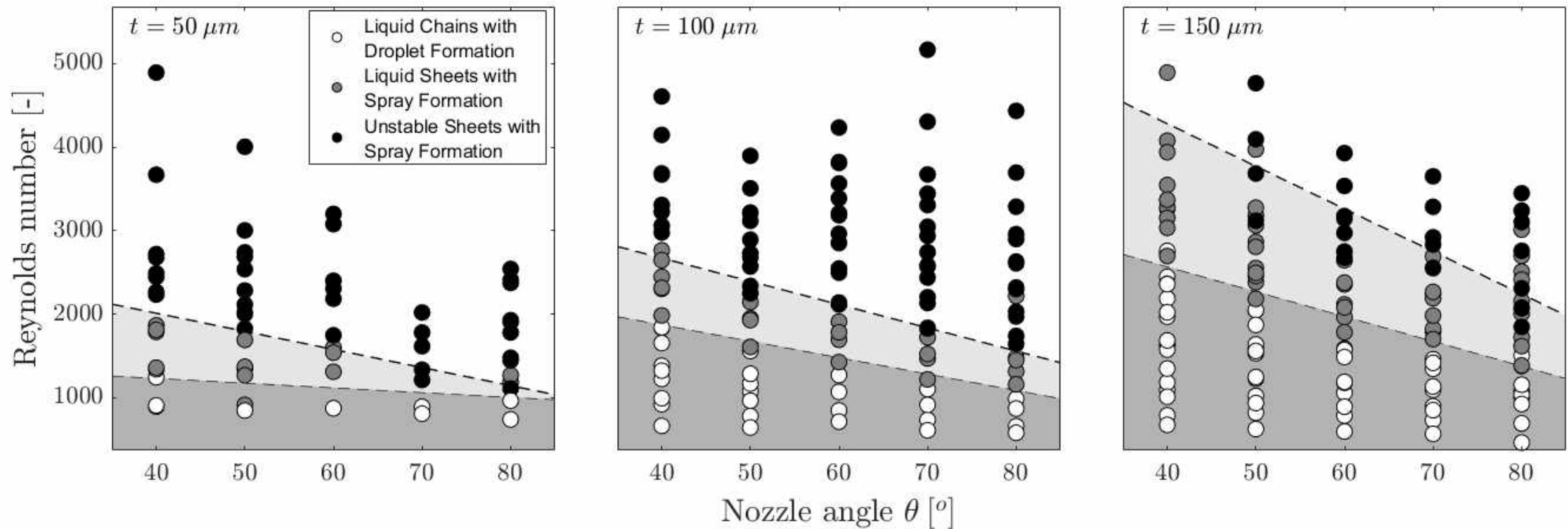
- Outlet defects - Shape deformation, Edge roughness & Wafer cracks
- Introduction of flow perturbations → Outliers presence





Sheet-breakup regime classification

- Nozzle thickness increase delaying spray formation
- Nozzle angle increase accelerating spray formation
- Linear regime boundaries – $Re = a + b\theta$





Presentation Outline

1. Introduction
2. Liquid sheets
3. Experimental Methods
4. Numerical Methods
5. Results
- 6. Summary and Conclusions**



Summary & Conclusions

- Design and development of a microfluidic device for liquid sheet generation
 - Lithographic fabrication of nozzle chips
 - Parametric study of fabrication, geometric and flow effects
- Evaluation of fabrication methods effects on sheet dynamics
- Sheet classification applying combined sheet and breakup patterns

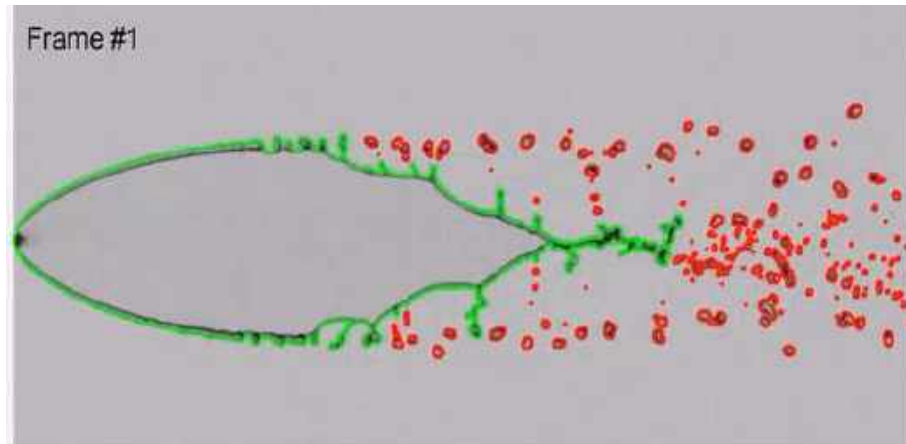


Summary & Conclusions

- Design and development of a microfluidic device for liquid sheet generation
 - Lithographic fabrication of nozzle chips
 - Parametric study of fabrication, geometric and flow effects
 - Evaluation of fabrication methods effects on sheet dynamics
 - Sheet classification applying combined sheet and breakup patterns
-
- Pronounced Q - and w_0 -effects on liquid sheet dimensions
 - Nozzle angle θ controlling sheet and rim stability
 - Drop-shedding rims at higher θ
 - Transition from jet- to spray-breakup
 - Critical influence of outlet polishing
 - Outlet dimensions modification
 - Sizing and stability features shift

Future Work

- Heat transfer efficiency for a flat surface using LS
- Heat transfer for a curved surface
- Study on the droplet dynamics



Developing a Microfluidic Nozzle to Generate Water Sheet Jets for Cooling Sharp Leading Edges

Priyanka Sinha

Thank you for your attention!

Questions?


Thermo Fluids
& Interfaces Lab



**DEPARTMENT OF
AEROSPACE ENGINEERING**

TECHNION
Israel Institute
of Technology



EFFECT ON THE THICKNESS

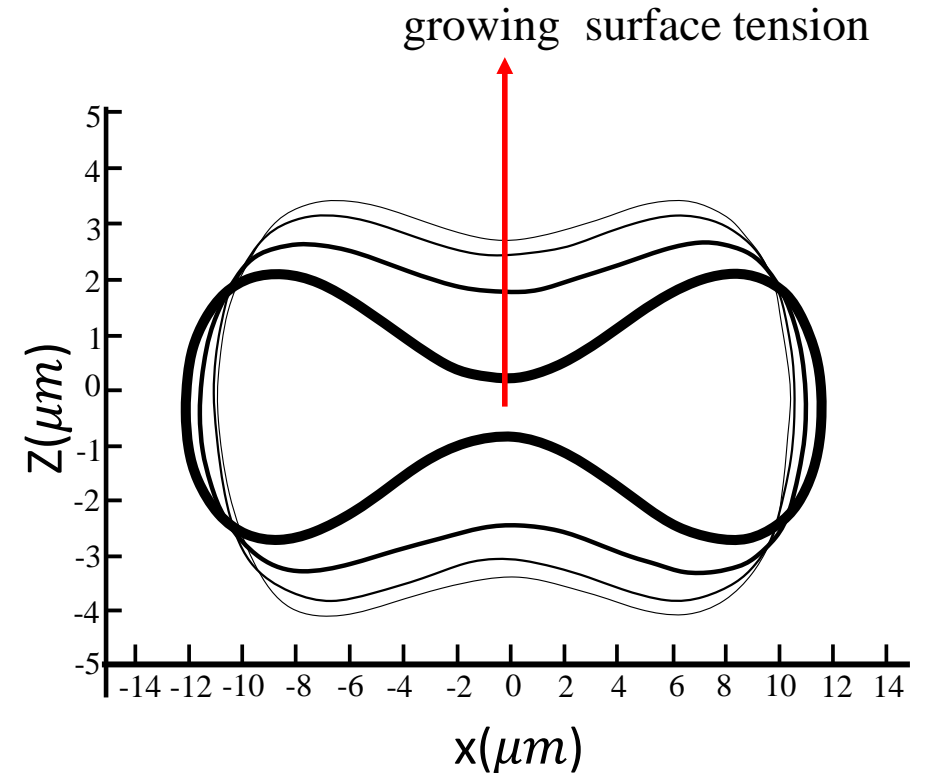
For thinner sheets:

- a) Increased impingement angle
- b) Working fluids
 - use of solvents
- c) Lower surface tension

Taylor: $h \propto 1/r$

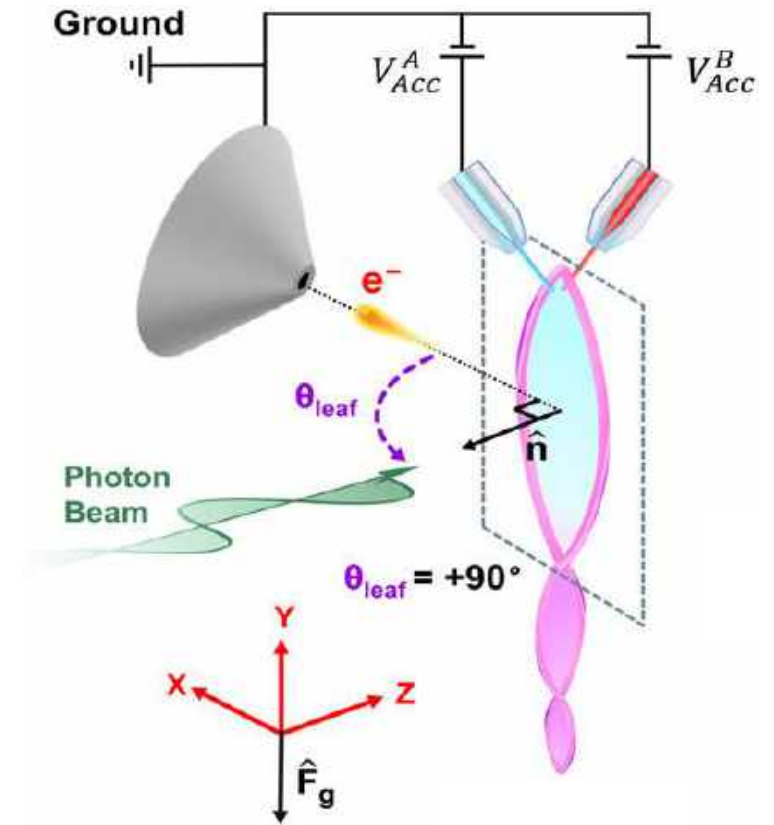
Hasson and Peck:
$$\frac{hr}{R_j^2} = \frac{\sin^3(\theta)}{\{1 - \cos(\phi)\cos(\theta)\}^2}$$

h-thickness of the sheet
r-radial distance
 ϕ -azimuthal angle



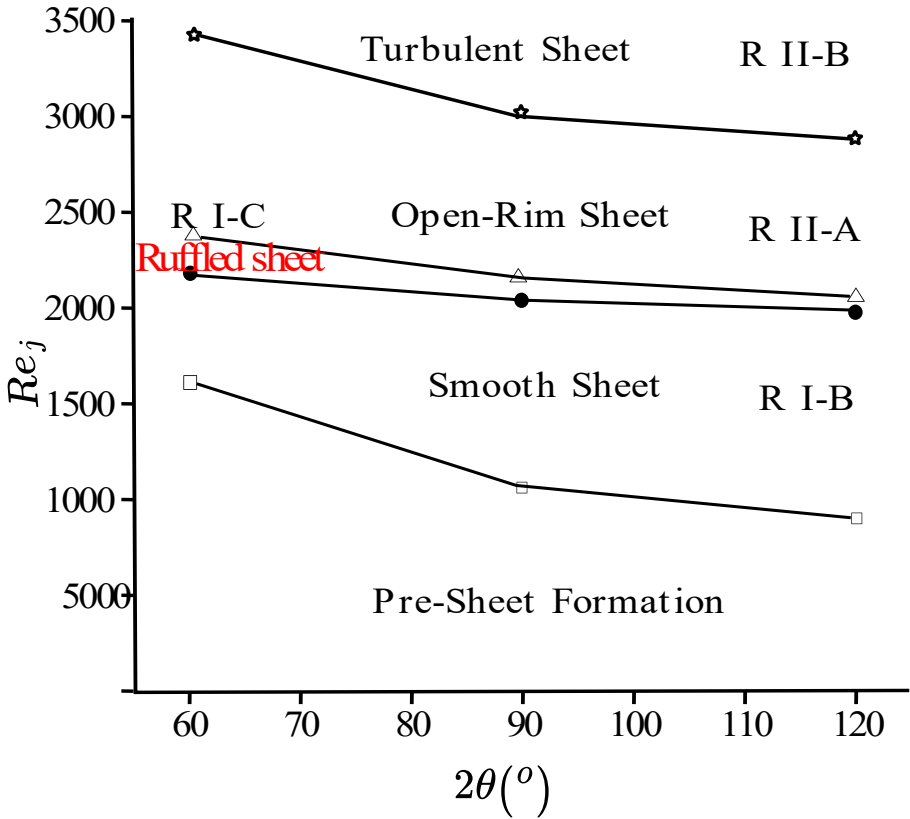
Application of LS

- X-ray, electron spectroscopy
- Fluid mixing in liquid propellants
- Chemical kinetics^[9]

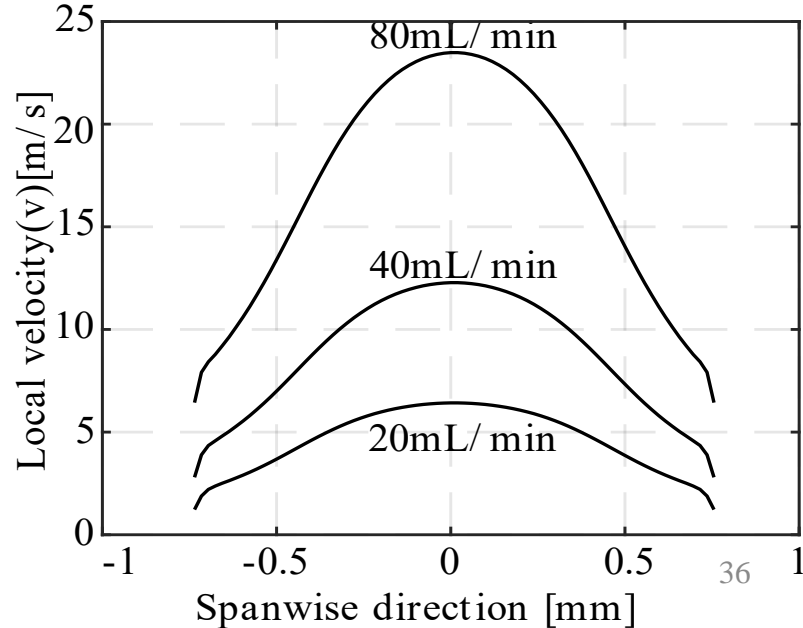
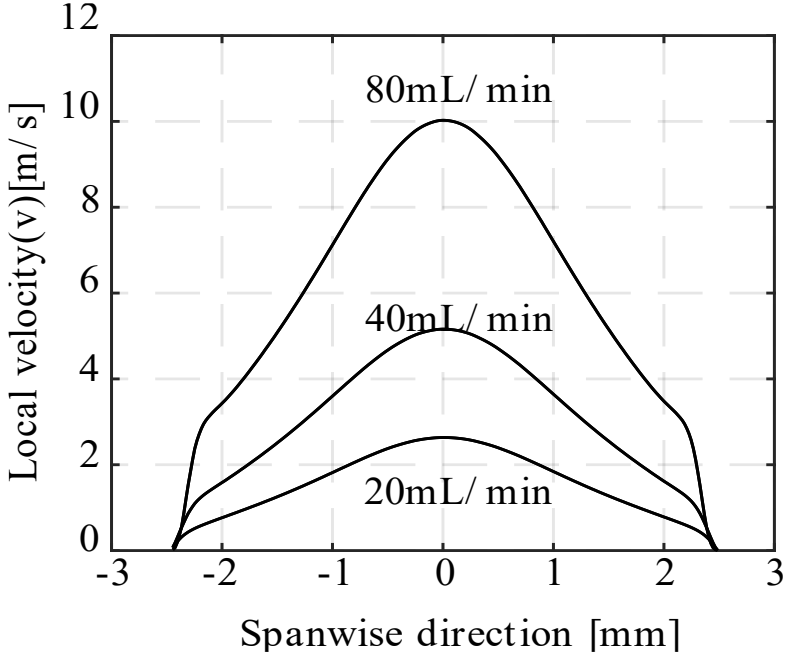


Liquid sheet used in
photoelectron spectroscopy
(PES)^[8]

Effect of Re on stability



Q variation –internal flow





CONTRIBUTING FACTORS

Aerodynamic waves

Hydrodynamic/impact waves

INSTABILITY PATTERN

Open rim w/o droplets

Closed rim w/ droplets

Open rim w/ droplets

Rimless sheet

Bow-shaped ligaments

Fully developed spray

DISINTERGATION MECHANISM

Jet impingement

Formation of flapping sheet

Evolution of ligaments

Eventual droplet formation